Ultrasonics Sonochemistry 82 (2022) 105898

Contents lists available at ScienceDirect

Ultrasonics Sonochemistry

journal homepage: www.elsevier.com/locate/ultson

Hydrodynamic cavitation efficiently inactivates potato virus Y in water

Arijana Filipić [a,*], Tadeja Lukežič [a], Katarina Bačnik [a,b], Maja Ravnikar [a], Meta Ješelnik [a], Tamara Košir [a], Martin Petkovšek [c], Mojca Zupanc [c], Matevž Dular [c], Ion Gutierrez Aguirre [a]

[a] Department of Biotechnology and Systems Biology, National Institute of Biology, Večna pot 111, 1000 Ljubljana, Slovenia
[b] Jožef Stefan International Postgraduate School, Jamova cesta 39, 1000 Ljubljana, Slovenia
[c] University of Ljubljana, Faculty of Mechanical Engineering, Aškerčeva 6, 1000 Ljubljana, Slovenia

ARTICLE INFO

Keywords:
Water decontamination
Virus inactivation
Potato virus Y
Hydrodynamic cavitation

ABSTRACT

Waterborne plant viruses can destroy entire crops, leading not only to high financial losses but also to food shortages. Potato virus Y (PVY) is the most important potato viral pathogen that can also affect other valuable crops. Recently, it has been confirmed that this virus is capable of infecting host plants via water, emphasizing the relevance of using proper strategies to treat recycled water in order to prevent the spread of the infectious agents. Emerging environmentally friendly methods such as hydrodynamic cavitation (HC) provide a great alternative for treating recycled water used for irrigation. In the experiments conducted in this study, laboratory HC based on Venturi constriction with a sample volume of 1 L was used to treat water samples spiked with purified PVY virions. The ability of the virus to infect plants was abolished after 500 HC passes, corresponding to 50 min of treatment under pressure difference of 7 bar. In some cases, shorter treatments of 125 or 250 passes were also sufficient for virus inactivation. The HC treatment disrupted the integrity of viral particles, which also led to a minor damage of viral RNA. Reactive species, including singlet oxygen, hydroxyl radicals, and hydrogen peroxide, were not primarily responsible for PVY inactivation during HC treatment, suggesting that mechanical effects are likely the driving force of virus inactivation. This pioneering study, the first to investigate eukaryotic virus inactivation by HC, will inspire additional research in this field enabling further improvement of HC as a water decontamination technology.

1. Introduction

Water scarcity is one of the most important problems we face today [1]. Reuse of different types of wastewater (raw influent, treated effluent or reclaimed water) has emerged as a contingency to cope with limited water availability in many regions of the world, and especially in regions with arid climates [2]. Such types of water can serve as a vector for the spread of pathogenic microorganisms, including viruses [3,4]. They can spread through water to a different extent, depending on their persistence within the aqueous environment, which is affected by a combination of biological (e.g., virus structure, presence of organic matter), physical (e.g., temperature, ultraviolet [UV] radiation), and chemical (e.g., pH, salts, antiviral agents) factors [5]. Water as a virus transmission route is particularly relevant in agriculture, as 70% of all water worldwide is used for irrigation [6]. Waterborne human pathogenic viruses can remain on infected plants and cause infections when consumed [7], while plant viruses can cause high crop losses [3]. This is particularly problematic in closed irrigation systems that recycle water, such as hydroponics, which are increasingly used in response to water scarcity, and enable transmission of plant viruses from one plant to another, where they can multiply and cause further crop infections [5].

Water has been confirmed to mediate in the transmission of various plant viruses, including resilient tobamoviruses such as cucumber green mottle mosaic virus [8]. Other tobamoviruses, including pepper mild mottle virus and tobacco mild green mosaic virus, have been shown to remain infectious after conventional wastewater treatment, exposing the potential risks of the uncontrolled use of recycled water for irrigation [9]. Waterborne transmission in an experimental hydroponic system has been confirmed for two other important plant viruses, pepino mosaic

Abbreviations: FFA, Furfuryl alcohol; HC, Hydrodynamic cavitation; MeOH, Methanol; Np, Hydrodynamic cavitation passes; PVY, Potato virus Y; ROS, Reactive oxygen species; RT-PCR, Reverse transcription polymerase chain reaction; RT-qPCR, Reverse transcription real-time polymerase chain reaction; TEM, Transmission electron microscopy; UV, Ultraviolet; COX, Cytochrome *c* oxidase.

* Corresponding author at: Večna pot 111, 1000 Ljubljana, Slovenia.
E-mail address: arijana.filipic@nib.si (A. Filipić).

https://doi.org/10.1016/j.ultsonch.2021.105898
Received 18 October 2021; Received in revised form 17 December 2021; Accepted 26 December 2021
Available online 28 December 2021

virus (*Potexvirus, Alphaflexiviridae*) and potato virus Y (PVY) (*Potyvirus, Potyviridae*), where viruses were transmitted from infected to healthy plants through nutrient solution [10]. The importance of PVY stems from its inclusion in the top 10 plant viruses from a scientific and economic perspective [11]. PVY is a filamentous RNA virus that is the most problematic virus of potato (*Solanum tuberosum L.*). Depending on the PVY strain, potato genotype and environmental conditions, PVY can cause different levels of infection with various outcomes, including potato yield losses of up to 85% [12]. Isolates from the recombinant PVY^{NTN} group are the most aggressive, affecting both potato leaves and tubers [13]. High losses in potato can be devastating as potato is one of the most important crops in the world [14]. PVY can also infect other relevant crops including tobacco, tomato and pepper [11].

To prevent the risk of virus transmission, recycled water used for irrigation must be properly disinfected, especially in closed irrigation systems. Various chemical (e.g., chlorination, ozonation), and physical (e.g., heat treatment, filtration, reverse osmosis, UV irradiation) methods are used to decontaminate irrigation water, but unfortunately all have some drawbacks. For instance, chlorination is problematic because it produces disinfection byproducts that are often cytotoxic, genotoxic, and/or carcinogenic [15], while UV irradiation can be significantly hindered by turbid and colored residues in the water. Heat treatment requires a lot of energy and filtration produces a lot of waste [16]. In recent years, novel environmentally friendly solutions have emerged, including cold plasma [17] and cavitation [18].

Cavitation is a phenomenon in which vapor bubbles (cavities) form in an initially homogeneous liquid medium due to a local drop in pressure. Hydrodynamic cavitation (HC) occurs in a liquid that is in motion where a submerged body or a flow tract itself (with its geometry) causes acceleration of the liquid resulting in a local pressure drop. When the pressure drops below the vaporization threshold, cavitation bubbles form [18]. When bubbles reach higher surrounding pressure, they collapse leading to extreme conditions provoking mechanical and chemical effects. The former include shock waves [19,20], microjets [21,22], shear forces [23], and pressure gradients in the microenvironment around the bubble [24]. Additionally, extreme temperatures [25] can result in chemical effects caused by homolysis of vaporous water molecules, leading to formation of reactive oxygen species (ROS), namely $^{\bullet}OH$ and $^{\bullet}H$ [26]. Physical changes in the microenvironment can mechanically disrupt organic material, including viruses, while the formation of ROS can affect it chemically, via oxidation. Both mechanisms can have the same result, deeming the organic material non-toxic (abiotic material) or non-infectious (biotic material) [18]. This is why cavitation can be used to treat waters polluted with various contaminants including pharmaceuticals [27–29], dyes [30], pesticides [31,32], cyanobacteria, fungi and bacteria (reviewed in [18,33]). Only few studies examined the effect of cavitation on viruses [34–36] and only one of these studies used HC [36]. Another study that mentioned viral inactivation with HC merely scratched the surface of this complex issue, as it only measured RNA degradation after HC treatment of rotaviruses without measuring changes in viral infectivity [37]. Since little information is available on viral inactivation with HC, its inactivation spectrum and mechanisms are still largely unknown.

In the present study, the inactivation of PVY^{NTN} in water by HC (Fig. 2) was investigated, making it the first study in the field of plant virus inactivation by HC and only the second on virus inactivation by HC in general. Furthermore, its pioneering approach also lies in the description of the modes of inactivation, as we examined the effect of HC on different virus components and assessed the role of chemical pathways, i.e. oxidation with ROS, on virus inactivation. For that purpose, we employed various methods including test plant infectivity assays, PCR-based techniques, transmission electron microscopy (TEM) and scavenger experiments. This study will help pave the way for important new research that will further improve the decontamination of recycled water used for irrigation, and by extension also of potable water, using this environmentally friendly method.

2. Materials and methods

2.1. Preparation of water samples

To study the effect of HC on PVY^{NTN} (hereafter referred to as PVY), water samples inoculated with purified viral particles were prepared. 1 L of tap water was spiked with 50 µL of purified PVY isolated from tobacco plants (*Nicotiana tabacum* cv. Xanthi) using a classical purification method that included saccharose and CsCl gradient ultracentrifugation [38]. Initial virus concentrations were determined by reverse transcription real-time PCR (RT-qPCR) as described in section 2.5.2 and ranged from 15.6 to 19.4 quantification cycles (Cqs), which corresponded to concentrations in the range of approximately 10^6 to 10^5 RNA copies / µL of sample, measured by RT-droplet digital PCR following the previously published protocol of Mehle et. al., 2018 [39].

2.2. HC device

Experiments were performed in a cavitation test rig first described by Zupanc et al., 2013 [40]. The basic design of the HC reactor consisted of a symmetrical Venturi constriction connected with two equal reservoirs (each with a volume of 2 L) and powered by a pressure difference between them (Fig. 1). Pressurized air pushed the sample from one reservoir to another (the passage of the sample in one direction took 6 s) through the constriction (1 mm high and 5 mm wide), where HC developed. In this way, the sample was exposed to the same cavitation conditions regardless of the direction. Passing the entire volume of water in one direction is defined as one HC pass. The pressure difference between the two reservoirs was maintained at 7 bar. These conditions were used for experiments 1–5 (Table 1). In experiment 6, the Venturi constriction was replaced by a channel with a geometry that prevented the formation of HC, and the pressure difference was lowered to 1.2 bar.

2.3. The experiments in HC device and control experiments

2.3.1. The experiments in HC device

In the present study, six separate experiments (Exp. 1–6) were conducted in the HC device using 1 L of inoculated water samples (Table 1). Four experiments were performed without (Exp. 1–3; 6) and two with the addition of scavengers (Exp. 4 and 5). Experiments 1–5 were conducted under the same HC conditions, while they were modified for experiment 6 (Table 1, Fig. 1). During the treatments, 10 – 12 mL representative aliquots were taken after 0, 125, 250 or 500 HC passes (Np), depending on the experiment (Table 1).

Scavenger experiments were conducted to determine whether PVY inactivation was a result of the chemical effects of HC. For OH radicals, 960 µL/L of methanol (>99.9%, Honeywell Riedel de Haen, Germany) was used as a scavenger [41], whereas for singlet oxygen ($^1O_2$), 100 µL/L furfuryl alcohol (FFA) (>97 %, Sigma-Aldrich, MO, USA) was used [42]. Scavengers were added to 1 L of inoculated water sample before HC treatment. In one of our previous studies, we determined that a certain concentration of a commonly used $^{\bullet}OH$ scavenger – salicylic acid, has a big impact on HC dynamics [26]. To confirm that HC characteristics were not affected by the selected concentration of scavengers in this study, visual observation of HC was performed using a high-speed camera Photron FastCam SA-Z (Fig. 2). Water samples with appropriate concentration of scavengers without PVY were used for this evaluation. No major differences between developed HC in water with or without scavengers were observed. To measure the formation of H_2O_2, which could have a role in virus inactivation, two additional experiments were performed under the same HC parameters as in Exp. 1–5, but without the addition of PVY. In these experiments, the presence of H_2O_2 was measured using semi-quantitative Quantofix Peroxide 25 test strips (Macherey-Nagel, Germany). Experiment 6, without Venturi constriction, served to determine whether virus inactivation was due to factors other than HC.

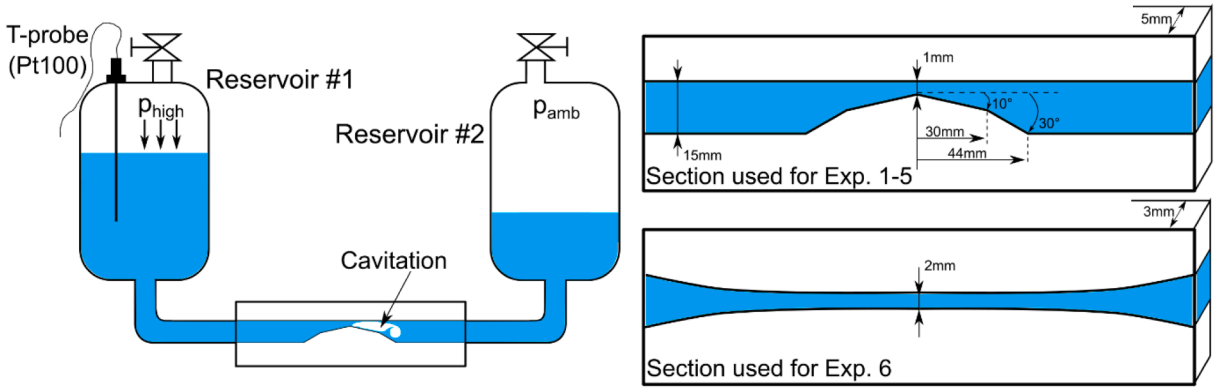

Fig. 1. Schematic representation of hydrodynamic cavitation test rig (left) with test section geometries used in experiments 1–5 and 6 (right).

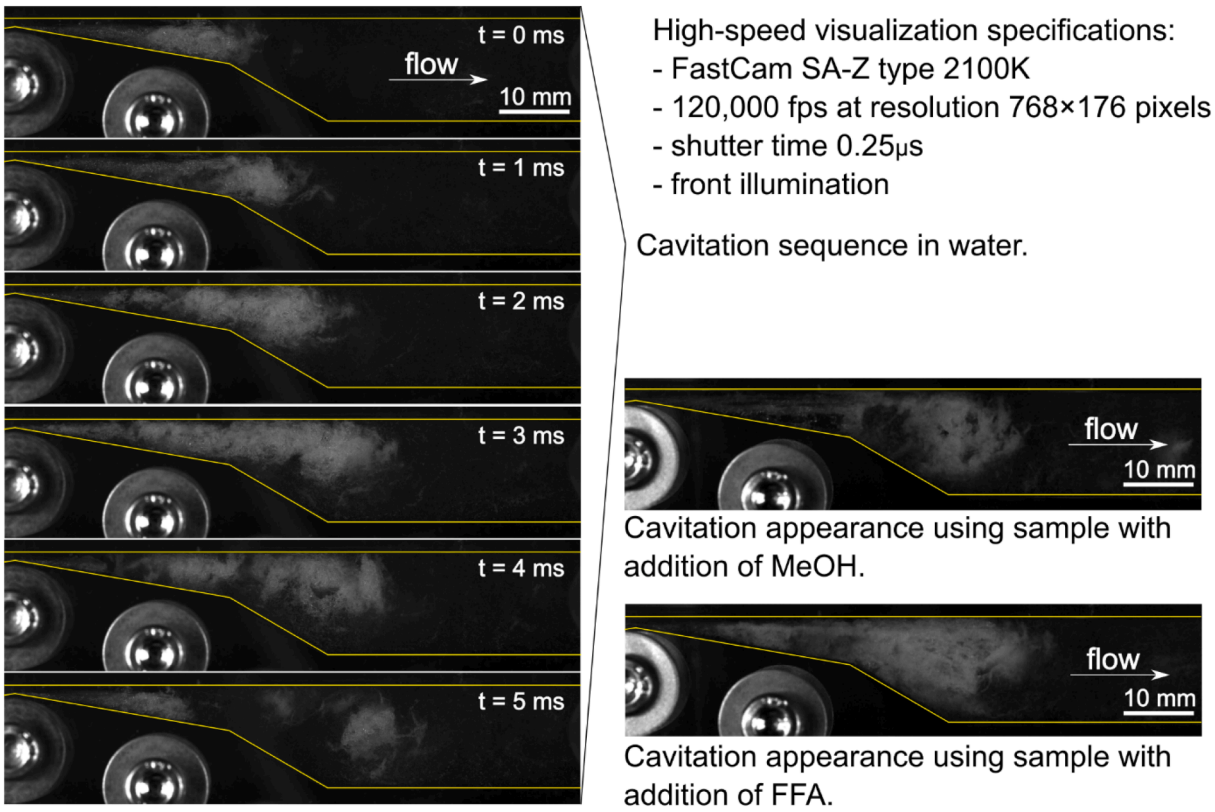

Fig. 2. Visualization of hydrodynamic cavitation (HC) in Venturi test section by high-speed camera in water samples without viruses. Visualization sequence of HC in water (left) and appearance of HC in water with scavengers: 960 μL/L of methanol (MeOH) and 100 μL/L of furfuryl alcohol (FFA) (right). Left side image represents a typical HC sequence developed in water, where periodic shedding of cavitation cloud can be observed. The cloud is growing from 0 to 3 ms, when it reaches its maximum size and starts to collapse from 3 to 5 ms. In time frame 5 ms the detached cavitation cloud can be seen. Right side images represent a typical HC appearance developed in water with scavengers at its maximum size, corresponding to time frame 3 ms in water without scavengers (left image). No major differences between developed HC were observed in water with or without scavengers.

After each experiment, sampled aliquots were stored on ice until used for test plant infectivity assays (Section 2.4) and TEM (Section 2.6), which was done the same day. If RNA extraction (Section 2.5.1) was not performed on the same day, aliquots were stored at −80° C. Aliquots collected at 0 Np served as positive controls of the infectivity assays, TEM and RT-PCR.

Temperature and pH were monitored during all experiments and measured using a Pt100 resistance temperature sensor, and a Hach-Lange HQ430d multimeter with PHC725 probe, respectively. The temperature of the samples never exceeded 36 °C during the experiments, while the pH was in the range from 7.3 to 8.3.

In order to avoid carryover of viruses between experiments, the reactor was cleaned with a washing protocol before and after each experiment. The protocol consisted of 10 Np with tap water, 100 Np with either 5% (v/v) Asepsol (Pliva, Croatia) or 2% (v/v) Incidin (Draeger, Germany), and 10 additional Np with tap water. The last step was repeated 6 times and fresh tap water was used each time.

2.3.2. *Control experiments*

To confirm that scavengers alone did not affect PVY infectivity, we performed three additional control experiments (Exp. 7–9) in a beaker on a magnetic stirrer (Table 1). Inoculated water samples were treated with each scavenger for 50 min (the approximate time span of Np = 500), and the last sample was just stirred, without the addition of

Table 1
Experimental design.

Exp.	HC	Virus	Sampling after Np				Scavenger	HC parameters	
			0	125	250	500		Constrictiongeometry	Pressuredifference
1	+	+	+	–	–	+	–	1 × 5 mm	7 bar
2	+	+	+	+	+	+	–		
3	+	+	+	+	+	+	–		
4	+	+	+	+	+	+	FFA		
5	+	+	+	+	+	+	MeOH		
6	–	+	+	+	+	+	–	2 × 3 mm	1.2 bar
7[a]	–	+	–	–	–	+	FFA	–	–
8[a]	–	+	–	–	–	+	MeOH	–	–
9[a]	–	+	–	–	–	+	–	–	–

HC, hydrodynamic cavitation; Np, number of HC passes; FFA, Furfuryl alcohol; MeOH, Methanol
[a] Control experiments performed on the magnetic stirrer

scavengers, and it served as a positive control of control experiments for the test plant infectivity assays.

2.4. Test plant infectivity assay

Test plant infectivity assays coupled with RT-qPCR were performed to determine if virus inactivation was achieved in experiments 1–9. Two leaves from at least four weeks old tobacco plants (*Nicotiana tabacum*, cv. 'White Burley') were dusted with carborundum dust to produce micro-injuries on the leaves. Dusted leaves of seven to eight plants were then carefully inoculated with a single aliquot (collected after 0, 125, 250, or 500 Np) by gently rubbing the leaves with the fingertip and rinsed with tap water after 7 min. Each experiment included a set of plants inoculated with tap water without virus, which served as a negative control of the test plant infectivity assays. Plants were grown in a quarantine greenhouse at 22 ± 2 °C during the 16-h light period and at 19 ± 2 °C during the 8-h dark period. Test plants were sampled twice, at least 14 and 28 days after inoculation. Plant material from 7 to 8 individual plants inoculated with the same aliquot was pooled and RNA extraction was performed. The RNeasy Plant Mini Kit (Qiagen, Germany) was used according to the manufacturer's instructions, with minor modifications, namely without using mercaptoethanol. A negative control of the extraction consisted of a sample of RNase-free water, which was co-extracted in each extraction batch, to observe for possible contaminations during the extraction process. Cytochrome c oxidase (COX) mRNA from the plant material served as an internal control of the extraction. The extracted RNA was then used in the RT-qPCR assays as described in section 2.5.2.

2.5. PCR-based methods

2.5.1. RT-PCR

RT-PCR was performed to examine the effects of HC on viral RNA degradation (Exp. 1–6). First, viral RNA was extracted from aliquots using the QIAmp Viral RNA Mini Kit (Qiagen), according to the manufacturer's instructions, with minor modifications including the addition of luciferase RNA (2 ng/sample) to the mixture of lysis buffer and carrier RNA as an external control of the extraction, and the final elution step was performed with 45 µL of RNase-free water. A sample of RNase-free water was included in each extraction round as a negative control of the extraction to monitor for potential contaminations during the procedure.

Extracted RNA was amplified using RT-PCR for four genes, e.g. P1, P3, NIaPRO and CP, as described in Filipić et al., 2019 [43]. Amplified PCR products were detected by 1% agarose gel electrophoresis and visualized with ethidium bromide. Their size was estimated using a 1-kb ladder. RNA was considered degraded if there was a notable decrease in at least two of the four amplified RNA regions.

2.5.2. RT-qPCR

RT-qPCR was used to detect virus replication in inoculated test plants after treatments, and to determine initial virus concentrations in the inoculated water samples. RNA was extracted from pooled plant tissue and from inoculated water samples using the RNAeasy Plant Mini Kit and the Viral RNA Mini Kit (both Qiagen), respectively, as described above. Three RT-qPCR assays were used: PVY-uni, LUC, and COX. Viral RNA was detected by PVY-uni assay [44] with 300 nM primers and 150 nM probe. The LUC assay [45] that contained 1000 nM primers and 500 nM probe targeted spiked luciferase RNA (used only for water samples), while the COX assay [10] targeted COX mRNA (used only for plant samples) and contained 900 nM primers and 200 nM probe. RT-qPCR assays were performed using the AgPath-ID One-Step RT-qPCR mix (Ambion, USA) as described by Filipić et al., 2019 [43] and Mehle et al., 2014 [10]. Each RT-qPCR run included a non-template control (sterilized water) and a previously extracted and characterized PVY RNA, which monitored for the contamination during the RT-qPCR process and success of amplification, respectively. RT-qPCR was carried out on an ABI Prism 7900HT Fast Detection system (Applied Biosystems, MA, USA) or a Viia 7 Real-Time system (Applied Biosystems), and results, i.e., Cq values, were acquired using SDS 2.4 software (Applied Biosystems) or QuantStudio Real-Time PCR software v 1.3 (Applied Biosystems). In each experiment, the results were considered positive, i.e., viruses were present in the plants, if the Cq values were lower than the lowest Cq value of all negative controls (e.g., the negative control of the test plant infectivity assays, the negative control of the extraction, and a non-template control) included in both samplings of the corresponding experiment (Supplementary material).

2.6. Transmission electron microscopy

The presence and morphology of PVY particles after the treatments in experiments 1–6 were determined by TEM using a negative staining method. 20 µL of sampled aliquots were applied to formvar-coated (Agar Scientific, Stansted, UK), carbon-stabilized copper grids that were negatively stained using a 1% (w/v) aqueous solution of uranyl acetate (SPI Supplies, West Chester, PA, USA). All samples were examined with TEM (Philips CM 100, Netherlands), operated at 80 kV and equipped with a CCD camera (Orius SC 200) and Digital Micrograph software (Gatan Inc., USA). Grids with an aliquot of 500 Np, Exp. 2, were not observed because viruses were no longer seen on the grids already after 250 Np.

3. Results and discussion

This is the first study on HC-mediated inactivation of an eukaryotic virus and only the second in the field of virus inactivation by HC, following up our previous study using bacteriophage MS2 as an enteric virus surrogate [36]. To the best of our knowledge, this is also the first study to investigate the modes of virus inactivation by HC and its effects

on different viral components, i.e., capsid and genome.

To assess virus inactivation by HC, five experiments, three without scavengers (Exp. 1–3) and two with scavengers (Exp. 4,5), were performed using inoculated water samples. High initial PVY concentrations were used and were of the same order of magnitude in all of these experiments, with Cq values ranging from 15.6 to 19.4. These concentrations are higher than the ones anticipated in hydroponic systems, where Cq values of 28 or more have been reported [10]. Table 2 shows that successful virus inactivation was achieved after 500 Np in all experiments, while in some experiments, even less Np were required (250 Np in Exp. 4 and 5, and 125 Np in Exp. 2). The difference in number of passes needed for inactivation may arise from the inherent variability of the test plant infectivity assays. Namely, the experiments were conducted throughout the year, and therefore the plants were grown at different times of the year, which may have affected their susceptibility to infection. In addition, some samples may have contained a small portion of damaged viruses before the treatment, which cannot be distinguished from undamaged ones by the RT-qPCR technique used here and are too few to be visible under the transmission electron microscope, but may still have an impact on virus infection. Experiments 6–9 showed that pushing the sample from one reservoir to another, addition of scavengers and stirring had no effect on virus inactivation, confirming that HC was the only responsible factor.

In addition to evaluating the inactivation potential of HC, we also wanted to determine if chemical effects of HC play any role in it. Therefore, we tested whether HC could inactivate PVY by oxidation with either of the two ROS, $^{\bullet}OH$ and $^{1}O_2$. Both $^{\bullet}OH$ and $^{1}O_2$ are strong, nonselective oxidants, which can oxidize all organic material, including lipids, proteins, and nucleic acids [46,47]. It has been suggested that $^{\bullet}OH$ was involved in MS2 inactivation during HC treatment, however this has not been confirmed by the empirical data [36]. On the other hand, $^{\bullet}OH$ has been shown to play an important role in the inactivation of MS2 [41,48] and adenovirus [49] in various non-cavitation treatments. Since it is difficult to directly measure the production of the various ROS due to their short lifespan [50], an indirect method with the addition of scavengers was employed. Despite the recent confirmation of $^{\bullet}OH$ presence in HC treated water [26], scavenging it with methanol did not prevent PVY inactivation suggesting that $^{\bullet}OH$ was not involved in virus inactivation during HC treatment (Table 2, experiment 5). Similar findings have been reported in other studies using different non-cavitation treatments, including cold atmospheric plasma and simulated sunlight in combination with different sensitizers, where the generated $^{\bullet}OH$ had no effect on the treated viruses, namely, feline calicivirus [51] and MS2 [52]. To the authors' knowledge, the formation of $^{1}O_2$ during cavitation has never been investigated, but could form under certain favorable conditions [53]. However, because $^{1}O_2$ has been shown to be crucial in other studies using non-cavitation techniques [51,52], we tested its impact on viruses during HC treatment. The results showed that the addition of the $^{1}O_2$ scavenger, FFA, did not prevent PVY inactivation, as seen in experiment 4 (Table 2). Even though H_2O_2 can form during cavitation [53], it did not form in sufficient concentrations in our HC setup to be detected by the Quantofix strips. Since none of the tested ROS (e.g., $^{\bullet}OH$, $^{1}O_2$, and H_2O_2) seemed to be involved in the PVY inactivation, it is very likely that the loss of its infectivity relies solely on the extreme mechanical events following the violent bubble collapses. Considering the filamentous PVY structure, the mechanical effects involved in inactivation most likely include the high-pressure gradients at the transition of the shockwaves, which are emitted during bubble collapses [24,54]. Petkovšek et al. [20] performed an experimental study on shockwaves emitted during cavitation cloud collapse on the same Venturi constriction as used in the present study. They showed that the magnitude of shockwaves exceeded several MPa, while reaching supersonic velocities, thus creating conditions that could be harsh enough to cause virus inactivation. Similarly, but for acoustic cavitation, Priyadarshi et al. [55] showed that shockwaves emitted at collapsing cavitation bubbles induced by an ultrasonic horn, also have a magnitude in the order of MPa and that they are most probably responsible for the fragmentation of solid intermetallic crystals. Since every structure, solid or not, has its own resonance frequency, they can be shattered by a frequency induced in the same frequency range. As viruses are extremely small, it can be presumed that their resonance frequency is very high, which also depends on their structure. In the study performed by Khavari et al. [56], it was shown that shockwaves emitted from a 24 kHz ultrasonic horn, resonate at a frequency in the order of MHz, which could be high enough to reach self-resonance frequency of the viruses. This could be the mechanism responsible for the inactivation of bacteriophages MS2 and ΦX174 investigated by Chrysikopoulos et al. [35]. They showed that viruses can be inactivated with different efficiency when using different ultrasonic frequencies. Even though these two viruses have a spherical structure (different to the filamentous structure of the PVY investigated in the present study), all these studies may serve as an indirect pointer that shockwaves play a role in the inactivation mechanisms of structurally different viruses. It is less likely that the damage would result from shear forces, which are too small at this scale, or micro jets, which could induce damage only at direct impingement of the virus.

Table 2
The effect of hydrodynamic cavitation treatment on viral infectivity and RNA.

Exp.	Scavenger	Virus inactivation after Np[a]			
		0	125	250	500
1	–	–	NA	NA	+
2	–	–	+	+	+
3	–	–	–	–	+
4	FFA	–	–	+	+[b]
5	MeOH	–	–	+	+[b]
6	–	–	–	–	–
7[c]	FFA	NA	NA	NA	–
8[c]	MeOH	NA	NA	NA	–
9[c]	–	NA	NA	NA	–

FFA, Furfuryl alcohol; MeOH, Methanol; NA, not applicable; Np, number of hydrodynamic cavitation passes

[a] Viruses were considered inactivated (+) if they were not detected by RT-qPCR in upper, systemic leaves collected and pooled from 7 or 8 inoculated plants after at least 14 and 28 days post inoculation

[b] In these two samples, RNA degradation was observed by RT-PCR

[c] Control experiments, performed on the magnetic stirrer.

Besides describing the effects of HC involved in inactivation, we also examined how they affect different viral components. Changes in viral particle morphology after HC treatments were observed by TEM. In all experiments, PVY was less damaged at the beginning of the experiment (Fig. 3A and D) and as the Np increased, the damage to the viral particles became more evident, with observed fragmentation and degradation (Fig. 3). Small circular structures on the surface of viral particles were observed in all samples (Fig. 3), which are usually not observed in PVY samples. Since their abundance increased with the higher Np, they could potentially be associated with PVY degradation. TEM results, where the observed degradation of viral particles increased with the increasing Np, coincided with the infectivity assay results. In samples treated for 500 Np, it was difficult to find and observe viral particles; only degraded virus parts or other artifacts were seen (Fig. 3G). In samples treated for less than 500 Np, where inactivation was confirmed with test plants, no viral particles or significantly damaged viruses were observed by TEM (Fig. 3F). In samples of low Np, where viruses remained infectious, undamaged viruses and viruses with differently pronounced damage were observed by TEM (Fig. 3B, C and E). Experiment 6, without HC treatment, had no effect on the virus integrity (Fig. 3H). Our TEM results clearly confirm that HC disrupts the integrity of the viral capsid, i.e., the outer protein layer of PVY.

The intact form of PVY virion building units is essential to retain viral infectivity [57]. PVY and all viruses in general require undamaged genetic material along with an intact protein capsid for successful infection

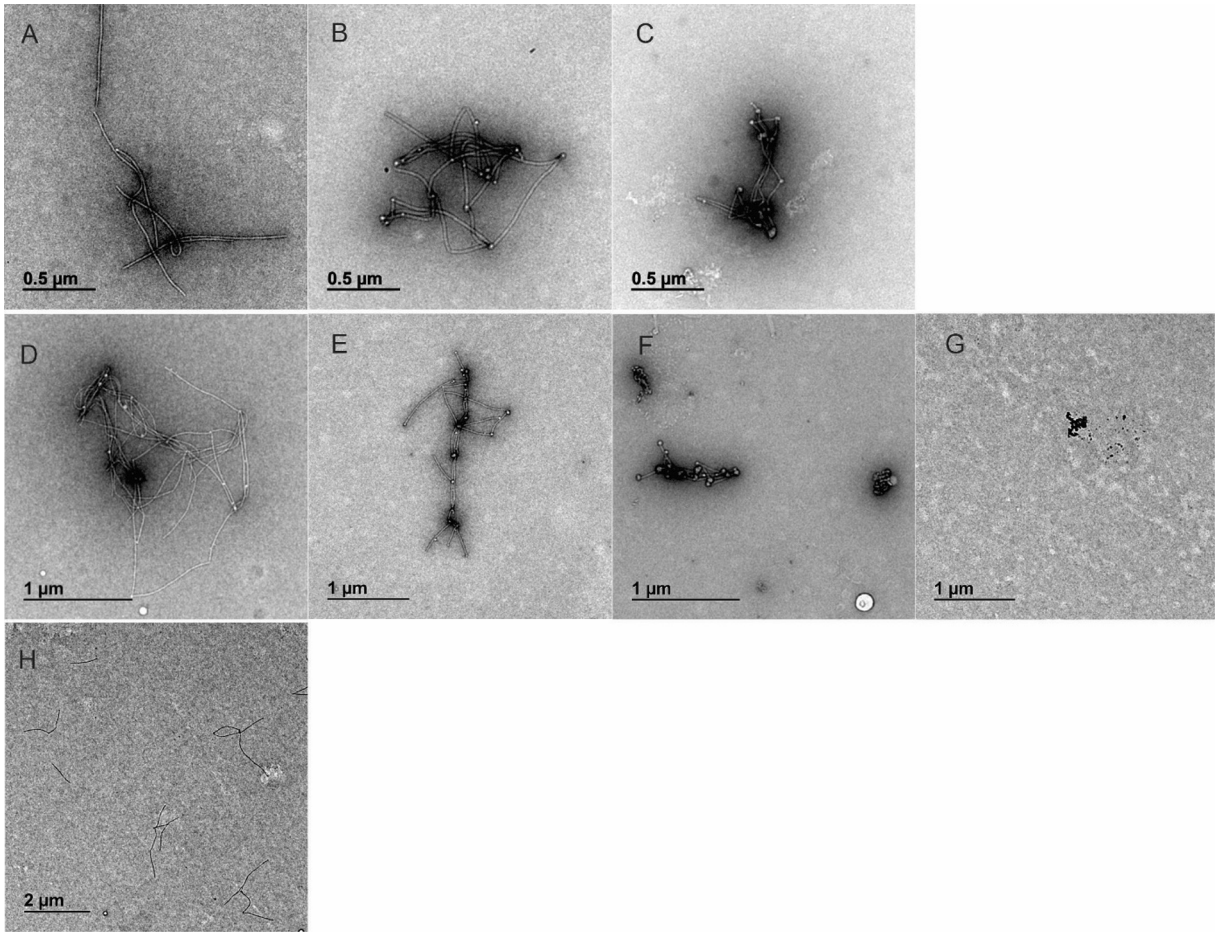

Fig. 3. Representative transmission electron microscopy micrographs of potato virus Y (PVY) in water during hydrodynamic cavitation (HC) experiments: 3 (A – C), 4 (D – G), and 6 (H). The highest number of whole viruses was observed in the untreated samples regardless of the experiment (A, D). With the increasing number of HC passes (Np), viral degradation was more pronounced, as seen after 125 (B, E) and 250 Np (C, F). After 500 Np, no viruses were observed, only some artifacts that may be connected to virus degradation (G). The addition of the scavenger furfuryl alcohol (experiment 4, D – G) had no effect on virus morphology as the observed viral degradation was similar to experiments without scavengers (for instance, experiment 3, A – C). In experiment 6, the number of viruses did not change with increasing Np and many intact viruses were still present after 500 Np (H). In panel H, viral particles are positively stained and thus seen as black filaments. The difference in magnification between the panels and therefore the difference in size of the viruses comes from the different scales (see scale bars).

and replication in host cells. Viruses with damaged genetic material can enter target cells but cannot replicate and thus pose no threat to the host organism [58]. To test whether HC can affect RNA degradation, we amplified four regions covering different parts of viral RNA using RT-PCR. In Exp. 4, and 5, minor RNA degradation was observed after 500 Np (a representative gel is shown in Fig. 4). In Exp. 6, no RNA

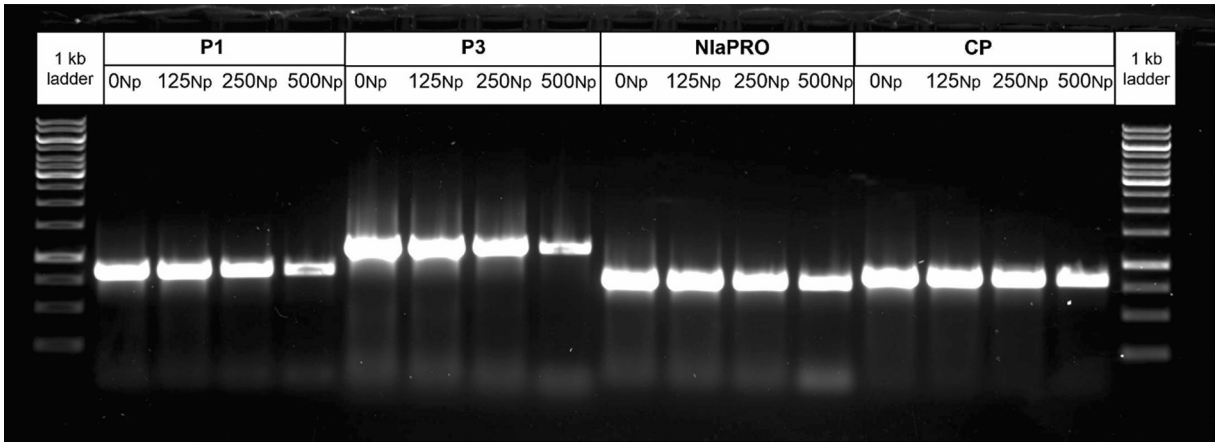

Fig. 4. Representative agarose gel showing RNA degradation of potato virus Y (PVY) after hydrodynamic cavitation (HC) treatment in experiment 5. RNA was marked as degraded if there was a notable change in at least two of four bands after the selected Np compared to the bands at time point 0. This was the case after 500 HC passes (Np) as minor degradation was observed for genes P1 and P3.

degradation was observed, indicating that the degradation was solely due to the HC treatment. Since viral particle damage increases with increasing Np, while RNA degradation was observed only in some prolonged HC treatments, RNA degradation appears to be preceded by disruption of capsid integrity, likely leaving viral RNA unprotected and accessible to the HC effect.

Up till now, only few studies have investigated virus inactivation by any type of cavitation. Feline calicivirus, murine norovirus, and bacteriophages φX147 and MS2 have been treated with acoustic cavitation [34,35], while HC has only been used to treat MS2 [36]. The concentration of infectious MS2 viruses was reduced by >4 logs after 1040 Np using a HC device similar to the one described here [36]. Because of the different approaches used to measure the inactivation of PVY and MS2 (test plant infectivity assay vs. double layer plaque assay), which provide quantitative results in the case of MS2 but only qualitative results in the case of PVY, it is impossible to directly compare the efficiency of inactivation of the two viruses. What we can conclude is that for PVY, 500 Np were needed to abolish the ability to infect plants of a relatively high concentration of the virus spiked in water, while for MS2, as mentioned above, 1040 Np resulted in a reduction of 4.8 logs in the amount of infective MS2 particles. The successful inactivation of these two different viruses with the similar HC device, consolidates the potential of HC as a tool for virus inactivation in water matrices. Since none of the above-mentioned studies investigated the mechanism of the HC-mediated inactivation, our results can serve as a cornerstone for further studies that will attempt to investigate whether the pattern we observed with PVY also occurs in the inactivation of a broader range of waterborne viruses. In addition, they may also help in describing the exact modes of viral inactivation by HC as is known for other water treatment technologies. For instance, chlorine and ozone usually damage the viral capsid rather than the nucleic acids, while UV irradiation mainly affects the nucleic acids, thereby preventing viruses from replicating [47]. Cold atmospheric plasma, a relatively new method for virus inactivation, can disrupt different viral components, including the lipid envelope, protein capsid, or nucleic acid, depending on the unique experimental properties (reviewed in [17]) and in the case of PVY, it can efficiently degrade RNA [43].

We have shown here that HC can successfully inactivate PVY in water samples after 500 Np or less. HC could thus help prevent the spread of important plant viruses such as PVY with recycled irrigation water (reclaimed wastewater and/or hydroponic nutrient solution). Our promising results will motivate extending the assessment of HC applicability to other plant viruses that can be transmitted by water including important pathogens such as cucumber green mottle mosaic virus, which has recently caused high losses in cucurbit crops [59], resulting in high economic losses. With the increasing use of closed irrigation systems in response to high irrigation water use and lack of fertile soil, the number of plant viruses spreading through water and causing plant infections and crop losses is likely to increase. Consequently, an environmentally friendly and efficient virus inactivation method such as HC would be highly beneficial tool to deploy among contingency measures to prevent such scenarios. Since the field of HC inactivation of viruses is still in its infancy, more work needs to be done to determine the range of HC inactivation capabilities as well as the exact mechanisms of inactivation in a broader range of viruses. In future studies, selection of different model viruses that require shorter times than plant viruses for completion of infectivity assays (i.e., 1–2 weeks, instead of 1–2 months) will allow us to fine tune the HC operating parameters with the aim of further improving virus inactivation. In addition, scaling up of the device, and its combination with other methods, which could further improve viral inactivation by shortening treatment times, also need to be explored.

4. Conclusions

In this study, inactivation of a plant virus PVY in water samples by HC was investigated. It was shown that inactivation can be achieved after a varying number of HC passes, ranging from 125 to 500, as demonstrated by test plant infectivity assays in conjunction with RT-qPCR. In addition to elucidating the efficiency of such inactivation, we sought to determine the mechanisms of virus inactivation. As observed by TEM and PCR-based methods, at the number of HC passes applied here, the damage to the protein capsid occurs more rapidly and severely than the damage to the genomic RNA, and therefore plays a leading role in PVY inactivation. Furthermore, strong oxidants, i.e., $^1O_2$, $^{\bullet}OH$, and H_2O_2, were shown not to be involved in virus inactivation, suggesting that PVY inactivation during HC treatment was likely due to extreme mechanical effects arising in the microenvironment around the collapsing bubbles, such as high-pressure gradients. Our results confirm that HC could be used as an alternative, environmentally friendly method for water decontamination that could successfully inactivate viruses without the use of chemicals or the production of toxic intermediates.

CRediT authorship contribution statement

Arijana Filipić: Conceptualization, Formal analysis, Writing – original draft. **Tadeja Lukežič:** Conceptualization, Formal analysis, Investigation, Writing – review & editing. **Katarina Bačnik:** Investigation, Writing – review & editing. **Maja Ravnikar:** Conceptualization, Writing – review & editing, Funding acquisition. **Meta Ješelnik:** Investigation, Writing – review & editing. **Tamara Košir:** Investigation, Writing – review & editing. **Martin Petkovšek:** Conceptualization, Investigation, Visualization, Writing – review & editing. **Mojca Zupanc:** Conceptualization, Investigation, Visualization, Writing – review & editing. **Matevž Dular:** Conceptualization, Visualization, Writing – review & editing, Supervision, Funding acquisition. **Ion Gutierrez Aguirre:** Conceptualization, Formal analysis, Writing – review & editing, Supervision.

Declaration of Competing Interest

The authors declare that they have no known competing financial interests or personal relationships that could have appeared to influence the work reported in this paper.

Acknowledgements

We thank Dr. Magda Tušek Žnidarič for her help with TEM results. The study was performed using Viia 7 Real-Time system financed by the Metrology Institute of the Republic of Slovenia (MIRS), with financial support from the European Regional Development Fund. This equipment is wholly owned by the Republic of Slovenia.

Funding sources.

This work was supported by the Slovenian Research Agency (Research Core Funding No. P4-0407, P2-0401, Projects No. L4-9325 and J7-1814), Ministry of Agriculture, Forestry and Food, Domžale-Kamnik Wastewater Treatment Plant and the European Research Council (ERC) under the European Union's Framework Program for research and innovation, Horizon 2020 (grant agreement No. 771567 — CABUM).

Appendix A. Supplementary data

Supplementary data to this article can be found online at https://doi.org/10.1016/j.ultsonch.2021.105898.

References

[1] World Economic Forum, The Global Risks Report (2019) 1–114.
[2] A.L. Thebo, P. Drechsel, E.F. Lambin, K.L. Nelson, A global, spatially-explicit assessment of irrigated croplands influenced by urban wastewater flows, Environ. Res. Lett. 12 (7) (2017) 074008, https://doi.org/10.1088/1748-9326/aa75d1.

[3] N. Mehle, M. Ravnikar, Plant viruses in aqueous environment - Survival, water mediated transmission and detection, Water Res. 46 (16) (2012) 4902–4917, https://doi.org/10.1016/j.watres.2012.07.027.

[4] S. Shrestha, S. Shrestha, J. Shindo, J.B. Sherchand, E. Haramoto, Virological quality of irrigation water sources and pepper mild mottle virus and tobacco mosaic virus as index of pathogenic virus contamination level, Food Environ. Virol. 10 (1) (2018) 107–120, https://doi.org/10.1007/s12560-017-9324-2.

[5] N. Mehle, I. Gutiérrez-Aguirre, D. Kutnjak, M. Ravnikar, Water-Mediated Transmission of Plant, Animal, and Human Viruses, Adv. Virus Res. 101 (2018) 85–128, https://doi.org/10.1016/bs.aivir.2018.02.004.

[6] United Nations World Water Assessment Programme/Un-Water (WWAP/ UNWater), The United Nations World Water Development Report 2018: Nature-Based Solutions for Water, 2018, 1-139.

[7] L. Maunula, A. Kaupke, P. Vasickova, K. Söderberg, I. Kozyra, S. Lazic, W.H.M. van der Poel, M. Bouwknegt, S. Rutjes, K.A. Willems, R. Moloney, M. D'Agostino, A. M. de Roda Husman, C.-H. von Bonsdorff, A. Rzeżutka, I. Pavlik, T. Petrovic, N. Cook, Tracing enteric viruses in the European berry fruit supply chain, Int. J. Food Microbiol. 167 (2) (2013) 177–185, https://doi.org/10.1016/j.ijfoodmicro.2013.09.003.

[8] J.-X. Li, S.-S. Liu, Q.-S. Gu, Transmission efficiency of cucumber green mottle mosaic virus via seeds, soil, pruning and irrigation water, J. Phytopathol. 164 (5) (2016) 300–309, https://doi.org/10.1111/jph.12457.

[9] K. Bačnik, D. Kutnjak, A. Pecman, N. Mehle, M. Tušek Žnidarič, I. Gutiérrez Aguirre, M. Ravnikar, Viromics and infectivity analysis reveal the release of infective plant viruses from wastewater into the environment, Water Res. 177 (2020) 115628, https://doi.org/10.1016/j.watres.2020.115628.

[10] N. Mehle, I. Gutiérrez-Aguirre, N. Prezelj, D. Delić, U. Vidic, M. Ravnikar, Survival and transmission of potato virus Y, pepino mosaic virus, and potato spindle tuber viroid in water, Appl. Environ. Microbiol. 80 (4) (2014) 1455–1462, https://doi.org/10.1128/AEM.03349-13.

[11] K.B.G. Scholthof, S. Adkins, H. Czosnek, P. Palukaitis, E. Jacquot, T. Hohn, B. Hohn, K. Saunders, T. Candresse, P. Ahlquist, C. Hemenway, G.D. Foster, Top 10 plant viruses in molecular plant pathology, Mol. Plant Pathol. 12 (2011) 938–954, https://doi.org/10.1111/j.1364-3703.2011.00752.x.

[12] Š. Baebler, A. Coll, K. Gruden, Plant Molecular responses to Potato Virus Y: a continuum of outcomes from sensitivity and tolerance to resistance, Viruses. 12 (2020) 217, https://doi.org/10.3390/v12020217.

[13] P. Kogovšek, M. Pompe-Novak, M. Petek, L. Fragner, W. Weckwerth, K. Gruden, K. Wu, Primary metabolism, phenylpropanoids and antioxidant pathways are regulated in potato as a response to potato virus Y infection, PLoS One. 11 (1) (2016) e0146135, https://doi.org/10.1371/journal.pone.0146135.

[14] FAOSTAT. http://www.fao.org/faostat/en/#data/QC/, 2003 (accessed 17 April 2021).

[15] B.A. Lyon, R.Y. Milsk, A.B. DeAngelo, J.E. Simmons, M.P. Moyer, H.S. Weinberg, Integrated chemical and toxicological investigation of UV-chlorine/ chloramine drinking water treatment, Environ. Sci. Technol. 48 (12) (2014) 6743–6753, https://doi.org/10.1021/es501412n.

[16] S.M. Stewart-Wade, Plant pathogens in recycled irrigation water in commercial plant nurseries and greenhouses: Their detection and management, Irrig. Sci. 29 (4) (2011) 267–297, https://doi.org/10.1007/s00271-011-0285-1.

[17] A. Filipić, I. Gutierrez-Aguirre, G. Primc, M. Mozetič, D. Dobnik, Cold plasma, a new hope in the field of virus inactivation, Trends Biotechnol. 38 (11) (2020) 1278–1291, https://doi.org/10.1016/j.tibtech.2020.04.003.

[18] M. Zupanc, Ž. Pandur, T. Stepišnik Perdih, D. Stopar, M. Petkovšek, M. Dular, Effects of cavitation on different microorganisms: The current understanding of the mechanisms taking place behind the phenomenon. A review and proposals for further research, Ultrason. Sonochem. 57 (2019) 147–165, https://doi.org/10.1016/j.ultsonch.2019.05.009.

[19] C.E. Brennen, Cavitation and Bubble Dynamics, Oxford University Press, Cambridge, 1995.

[20] M. Petkovšek, M. Hočevar, M. Dular, Visualization and measurements of shock waves in cavitating flow, Exp. Therm. Fluid Sci. 119 (2020) 110215, https://doi.org/10.1016/j.expthermflusci.2020.110215.

[21] G.L. Chahine, C.-T. Hsiao, Modelling cavitation erosion using fluid–material interaction simulations, Interface Focus. 5 (5) (2015) 20150016, https://doi.org/10.1098/rsfs.2015.0016.

[22] M. Dular, T. Požar, J. Zevnik, R. Petkovšek, High speed observation of damage created by a collapse of a single cavitation bubble, Wear. 418–419 (2019) 13–23, https://doi.org/10.1016/j.wear.2018.11.004.

[23] S.R. Gonzalez-Avila, A.C. van Blokland, Q. Zeng, C.-D. Ohl, Cavitation Bubble Collapse and Wall Shear Stress Generated in a Narrow Gap, in: J. Katz (Ed.), Proc. 10th Int. Symp. Cavitation, ASME Press, 2018: pp. 172–178. https://doi.org/10.1115/1.861851_ch34.

[24] J. Zevnik, M. Dular, Cavitation bubble interaction with a rigid spherical particle on a microscale, Ultrason. Sonochem. 69 (2020) 105252, https://doi.org/10.1016/j.ultsonch.2020.105252.

[25] K.S. Suslick, N.C. Eddingsaas, D.J. Flannigan, S.D. Hopkins, H. Xu, Extreme conditions during multibubble cavitation: Sonoluminescence as a spectroscopic probe, Ultrason. Sonochem. 18 (4) (2011) 842–846, https://doi.org/10.1016/j.ultsonch.2010.12.012.

[26] M. Zupanc, M. Petkovšek, J. Zevnik, G. Kozmus, A. Šmid, M. Dular, Anomalies detected during hydrodynamic cavitation when using salicylic acid dosimetry to measure radical production, Chem. Eng. J. 396 (2020) 125389, https://doi.org/10.1016/j.cej.2020.125389.

[27] P. Thanekar, M. Panda, P.R. Gogate, Degradation of carbamazepine using hydrodynamic cavitation combined with advanced oxidation processes, Ultrason. Sonochem. 40 (2018) 567–576, https://doi.org/10.1016/j.ultsonch.2017.08.001.

[28] M. Zupanc, T. Kosjek, M. Petkovšek, M. Dular, B. Kompare, B. Širok, M. Stražar, E. Heath, Shear-induced hydrodynamic cavitation as a tool for pharmaceutical micropollutants removal from urban wastewater, Ultrason. Sonochem. 21 (3) (2014) 1213–1221, https://doi.org/10.1016/j.ultsonch.2013.10.025.

[29] S. Rajoriya, S. Bargole, S. George, V.K. Saharan, P.R. Gogate, A.B. Pandit, Synthesis and characterization of samarium and nitrogen doped TiO2 photocatalysts for photo-degradation of 4-acetamidophenol in combination with hydrodynamic and acoustic cavitation, Sep. Purif. Technol. 209 (2019) 254–269, https://doi.org/10.1016/j.seppur.2018.07.036.

[30] E. Cako, K.D. Gunasekaran, R.D. Cheshmeh Soltani, G. Boczkaj, Ultrafast degradation of brilliant cresyl blue under hydrodynamic cavitation based advanced oxidation processes (AOPs), Water Resour. Ind. 24 (2020) 100134, https://doi.org/10.1016/j.wri.2020.100134.

[31] D. Panda, S. Manickam, Hydrodynamic cavitation assisted degradation of persistent endocrine-disrupting organochlorine pesticide Dicofol: Optimization of operating parameters and investigations on the mechanism of intensification, Ultrason. Sonochem. 51 (2019) 526–532, https://doi.org/10.1016/j.ultsonch.2018.04.003.

[32] P. Thanekar, P. Murugesan, P.R. Gogate, Improvement in biological oxidation process for the removal of dichlorvos from aqueous solutions using pretreatment based on Hydrodynamic Cavitation, J. Water Process Eng. 23 (2018) 20–26, https://doi.org/10.1016/j.jwpe.2018.03.004.

[33] P.R. Gogate, Application of cavitational reactors for water disinfection: Current status and path forward, J. Environ. Manage. 85 (4) (2007) 801–815, https://doi.org/10.1016/j.jenvman.2007.07.001.

[34] X. Su, S. Zivanovic, D.H. D'Souza, Inactivation of Human Enteric Virus Surrogates by High-Intensity Ultrasound, Foodborne Pathog. Dis. 7 (9) (2010) 1055–1061, https://doi.org/10.1089/fpd.2009.0515.

[35] C.V. Chrysikopoulos, I.D. Manariotis, V.I. Syngouna, Virus inactivation by high frequency ultrasound in combination with visible light, Colloids Surfaces B Biointerfaces. 107 (2013) 174–179, https://doi.org/10.1016/j.colsurfb.2013.01.038.

[36] J. Kosel, I. Gutiérrez-Aguirre, N. Rački, T. Dreo, M. Ravnikar, M. Dular, Efficient inactivation of MS-2 virus in water by hydrodynamic cavitation, Water Res. 124 (2017) 465–471, https://doi.org/10.1016/j.watres.2017.07.077.

[37] M. Dular, T. Griessler-Bulc, I. Gutierrez-Aguirre, E. Heath, T. Kosjek, A. Krivograd Klemenčič, M. Oder, M. Petkovšek, N. Rački, M. Ravnikar, A. Šarc, B. Širok, M. Zupanc, M. Žitnik, B. Kompare, Use of hydrodynamic cavitation in (waste)water treatment, Ultrason. Sonochem. 29 (2016) 577–588, https://doi.org/10.1016/j.ultsonch.2015.10.010.

[38] M. Rupar, M. Ravnikar, M. Tušek-Žnidarič, P. Kramberger, L. Glais, I. Gutiérrez-Aguirre, Fast purification of the filamentous Potato virus Y using monolithic chromatographic supports, J. Chromatogr. A. 1272 (2013) 33–40, https://doi.org/10.1016/j.chroma.2012.11.058.

[39] N. Mehle, D. Dobnik, M. Ravnikar, M. Pompe Novak, Validated reverse transcription droplet digital PCR serves as a higher order method for absolute quantification of Potato virus Y strains, Anal. Bioanal. Chem. 410 (16) (2018) 3815–3825, https://doi.org/10.1007/s00216-018-1053-3.

[40] M. Zupanc, T. Kosjek, M. Petkovšek, M. Dular, B. Kompare, B. Širok, Ž. Blažeka, E. Heath, Removal of pharmaceuticals from wastewater by biological processes, hydrodynamic cavitation and UV treatment, Ultrason. Sonochem. 20 (4) (2013) 1104–1112, https://doi.org/10.1016/j.ultsonch.2012.12.003.

[41] M. Cho, H. Chung, W. Choi, J. Yoon, Different inactivation behaviors of MS-2 phage and Escherichia coli in TiO2 photocatalytic disinfection, Appl. Environ. Microbiol. 71 (1) (2005) 270–275, https://doi.org/10.1128/AEM.71.1.270-275.2005.

[42] C.-Y. Chen, C.T. Jafvert, Photoreactivity of carboxylated single-walled carbon nanotubes in sunlight: Reactive oxygen species production in water, Environ. Sci. Technol. 44 (17) (2010) 6674–6679, https://doi.org/10.1021/es101073p.

[43] A. Filipić, G. Primc, R. Zaplotnik, N. Mehle, I. Gutierrez-Aguirre, M. Ravnikar, M. Mozetič, J. Žel, D. Dobnik, Cold Atmospheric plasma as a novel method for inactivation of potato virus Y in water samples, Food Environ. Virol. 11 (3) (2019) 220–228, https://doi.org/10.1007/s12560-019-09388-y.

[44] P. Kogovšek, L. Gow, M. Pompe-Novak, K. Gruden, G.D. Foster, N. Boonham, M. Ravnikar, Single-step RT real-time PCR for sensitive detection and discrimination of Potato virus Y isolates, J. Virol. Methods. 149 (1) (2008) 1–11, https://doi.org/10.1016/j.jviromet.2008.01.025.

[45] N. Toplak, V. Okršlar, D. Stanič-Racman, K. Gruden, J. Žel, A high-throughput method for quantifying transgene expression in transformed plants with real-time PCR analysis, Plant Mol. Biol, Report. 22 (3) (2004) 237–250, https://doi.org/10.1007/BF02773134.

[46] P. Di Mascio, G.R. Martinez, S. Miyamoto, G.E. Ronsein, M.H.G. Medeiros, J. Cadet, Singlet molecular oxygen reactions with nucleic acids, lipids, and proteins, Chem. Rev. 119 (3) (2019) 2043–2086, https://doi.org/10.1021/acs.chemrev.8b00554.

[47] B.K. Mayer, Y. Yang, D.W. Gerrity, M. Abbaszadegan, The Impact of capsid proteins on virus removal and inactivation during water treatment processes, Microbiol. Insights. 8 (2015) 15–28, https://doi.org/10.4137/MBI.S31441.

[48] S. Rattanakul, K. Oguma, Analysis of hydroxyl radicals and inactivation mechanisms of bacteriophage MS2 in Response to a simultaneous application of UV and chlorine, Environ. Sci. Technol. 51 (1) (2017) 455–462, https://doi.org/10.1021/acs.est.6b0339410.1021/acs.est.6b03394.s001.

[49] S. Bounty, R.A. Rodriguez, K.G. Linden, Inactivation of adenovirus using low-dose UV/H2O2 advanced oxidation, Water Res. 46 (19) (2012) 6273–6278, https://doi.org/10.1016/j.watres.2012.08.036.
[50] K.K. Griendling, R.M. Touyz, J.L. Zweier, S. Dikalov, W. Chilian, Y.-R. Chen, D. G. Harrison, A. Bhatnagar, Measurement of reactive oxygen species, reactive nitrogen species, and redox-dependent signaling in the cardiovascular System: A Scientific statement from the american heart association, Circ. Res. 119 (2016) 139–148, https://doi.org/10.1161/RES.0000000000000110.
[51] H.A. Aboubakr, U. Gangal, M.M. Youssef, S.M. Goyal, P.J. Bruggeman, Inactivation of virus in solution by cold atmospheric pressure plasma: identification of chemical inactivation pathways, J. Phys. D, Appl. Phys. 49 (20) (2016) 204001, https://doi.org/10.1088/0022-3727/49/20/204001.
[52] T. Kohn, K.L. Nelson, Sunlight-mediated inactivation of MS2 coliphage via exogenous singlet oxygen produced by sensitizers in natural waters, Environ. Sci. Technol. 41 (1) (2007) 192–197, https://doi.org/10.1021/es061716i10.1021/es061716i.s001.
[53] I.P. Ivanova, S.V. Trofimova, I.M. Piskarev, N.A. Aristova, O.E. Burhina, O. O. Soshnikova, Mechanism of chemiluminescence in Fenton reaction, J. Biophys. Chem. 03 (01) (2012) 88–100, https://doi.org/10.4236/jbpc.2012.31011.
[54] J. Zevnik, M. Dular, Liposome destruction by a collapsing cavitation micro bubble: A numerical study, Ultrason. Sonochem. 78 (2021) 105706, https://doi.org/10.1016/j.ultsonch.2021.105706.
[55] A. Priyadarshi, M. Khavari, S. Bin Shahrani, T. Subroto, L.A. Yusuf, M. Conte, P. Prentice, K. Pericleous, D. Eskin, I. Tzanakis, In-situ observations and acoustic measurements upon fragmentation of free-floating intermetallics under ultrasonic cavitation in water, Ultrason. Sonochem. 80 (2021) 105820, https://doi.org/10.1016/j.ultsonch.2021.105820.
[56] M. Khavari, A. Priyadarshi, A. Hurrell, K. Pericleous, D. Eskin, I. Tzanakis, Characterization of shock waves in power ultrasound, J. Fluid Mech. 915 (2021), https://doi.org/10.1017/jfm.2021.186.
[57] A. Kežar, L. Kavčič, M. Polák, J. Nováček, I. Gutiérrez-Aguirre, M.T. Žnidarič, A. Coll, K. Stare, K. Gruden, M. Ravnikar, D. Pahovnik, E. Žagar, F. Merzel, G. Anderluh, M. Podobnik, Structural basis for the multitasking nature of the potato virus Y coat protein, Sci. Adv. 5 (2019) eaaw3808, https://doi.org/10.1126/sciadv.aaw3808.
[58] R. Hull, Comparative plant virology, Elsevier Inc., Burlington, MA, USA, 2009.
[59] A. Dombrovsky, L.T.T. Tran-Nguyen, R.A.C. Jones, Cucumber green mottle mosaic virus: rapidly increasing global distribution, etiology, epidemiology, and management, Annu. Rev. Phytopathol. 55 (1) (2017) 231–256, https://doi.org/10.1146/phyto.2017.55.issue-110.1146/annurev-phyto-080516-035349.